

# Photoencapsulation of osteoblasts in injectable RGD-modified PEG hydrogels for bone tissue engineering

Jason A. Burdick<sup>a</sup>, Kristi S. Anseth<sup>a,b,\*</sup>

<sup>a</sup>Department of Chemical Engineering, University of Colorado, Campus Box 424, Engineering Center, ECCH 111, Boulder, CO 80309-0424, USA

<sup>b</sup>Howard Hughes Medical Institute, University of Colorado, Boulder, CO 80309-0424, USA

Received 16 October 2001; accepted 4 January 2002

## Abstract

Poly(ethylene glycol) (PEG) hydrogels were investigated as encapsulation matrices for osteoblasts to assess their applicability in promoting bone tissue engineering. Non-adhesive hydrogels were modified with adhesive Arg-Gly-Asp (RGD) peptide sequences to facilitate the adhesion, spreading, and, consequently, cytoskeletal organization of rat calvarial osteoblasts. When attached to hydrogel surfaces, the density and area of osteoblasts attached were dramatically different between modified and unmodified hydrogels. A concentration dependence of RGD groups was observed, with increased osteoblast attachment and spreading with higher RGD concentrations, and cytoskeleton organization was seen with only the highest peptide density. A majority of the osteoblasts survived the photoencapsulation process when gels were formed with 10% macromer, but a decrease in osteoblast viability of ~25% and 38% was seen after 1 day of in vitro culture when the macromer concentration was increased to 20 and 30 wt%, respectively. There was no statistical difference in cell viability when peptides were added to the network. Finally, mineral deposits were seen in all hydrogels after 4 weeks of in vitro culture, but a significant increase in mineralization was observed upon introduction of adhesive peptides throughout the network. © 2002 Elsevier Science Ltd. All rights reserved.

**Keywords:** Photoencapsulation; RGD; Bone tissue engineering; Injectable; Osteoblasts

## 1. Introduction

Injuries and diseases related to the musculoskeletal system plague millions of individuals each year. In many instances, a large defect remains that must be treated to restore original function to the bone. While autograft procedures, where bone is removed from one area of the patient's skeleton and implanted into the defect, are considered by many orthopedic surgeons to be the best option for treating large bone defects, these procedures still have many limitations [1]. For instance, bone grafting requires a second surgical site, is limited in quantity, and is restricted regarding the integration of implanted bone and vascular structures with native tissue. As an alternative approach, tissue engineering

may overcome these limitations. However, tissue engineering of bone requires identification of a suitable osteoconductive matrix that may be designed to include the release of osteoinductive factors or the delivery of osteoprogenitor cells [2,3]. Traditionally, the osteoconductive matrix is a prefabricated 3-dimensional scaffold composed of degradable polymers or ceramics, but an in situ forming scaffold may provide many advantages.

With in situ forming scaffolds, the ex vivo fabrication of complicated scaffold geometries is eliminated, which is often difficult due to the complexity of the defect site, and in situ forming scaffolds can improve contact between the scaffold and surrounding tissue. Poly(methyl methacrylate) (PMMA) bone cements are perhaps the most widely used injectable and in situ forming materials used in orthopedics. PMMA cements are applied by mixing a polymer powder, containing an initiator, with a monomer liquid to initiate polymerization of the resulting slurry at room temperature. While successful in many aspects of their application, these cements are limited by extreme exothermic temperature

\*Corresponding author. Department of Chemical Engineering, University of Colorado, Campus Box 424, Engineering Center, ECCH 111, Boulder, CO 80309-0424, USA. Tel.: +1-303-492-3147; fax: +1-303-492-4391.

E-mail address: kristi.anseth@colorado.edu (K.S. Anseth).

risers during polymerization that can lead to necrosis of surrounding tissues and implant failure [4]. Furthermore, PMMA is non-degradable and, thus, a permanent foreign material remains in the body, which may impede bone healing. The development and use of injectable orthopedic biomaterials that are degradable and polymerize under controlled conditions would provide numerous benefits as a non-invasive alternative to current treatment options for debilitating orthopedic conditions.

With this in mind, investigators have developed highly crosslinked, in situ forming degradable networks such as poly(propylene fumarates) [5,6] and polyanhydrides [7,8]. These hydrophobic networks are able to form directly in the body using either a thermal or photo-initiated polymerization. In particular, the controllable nature of photopolymerizations allows for temporal control of the reaction and, thus, minimization of exothermic temperature rises [9]. Although there are many advantages to these materials, such as their osteoconductive properties, mechanics, and controlled degradation behavior, the delivery of osteoprogenitor cells to defects is limited because the networks are too highly crosslinked to maintain cell viability. One alternative to these high-strength, hydrophobic networks is to encapsulate osteoblasts in hydrophilic networks that can be delivered directly to the defect site through injection and in situ polymerization.

Highly swollen hydrogels are capable of suspending cells 3-dimensionally and supporting nutrient diffusion to encapsulated cells, but may not provide an ideal environment for anchorage-dependent osteoblasts. Specifically, the attachment of various peptides to biomaterial surfaces has enhanced the adhesion of osteoblasts [10,11] and may promote an enhanced biomimetic environment for encapsulated cells suspended in 3-dimensional hydrogels. The most commonly researched adhesive peptide, Arg-Gly-Asp (RGD), is found in cell-binding domains of extracellular matrix proteins. Integrins on the surface of cells bind to the RGD and allow cells to adhere to otherwise non-adhesive surfaces.

Although extensive research has been done on *cell-surface* interactions with peptide modified biomaterials, the development of 3-dimensional hydrogels that contain peptide groups is limited. Specifically, RGD groups have been incorporated into alginate gels [12], *N*-isopropylacrylamide and acrylic acid hydrogels [13], and poly(ethylene glycol) (PEG) hydrogels [14,15]. These investigators have shown methods to 3-dimensionally incorporate adhesive ligands into networks and the benefits of RGD ligands on cell functions, such as adhesion and spreading. The overall objective of this work is to utilize previously developed chemistries to tether RGD to PEG-based hydrogels [14], and address issues that are particularly important to the design of an

in situ forming scaffold for bone tissue engineering. Specifically, we aim to answer the following fundamental questions related to the photoencapsulation of osteoblasts in hydrogel materials: (1) Do osteoblasts remain viable after photoencapsulation and during extended cultures? (2) Will photoencapsulated osteoblasts produce a mineralized extracellular matrix in a hydrogel environment? and (3) Will tethered RGD ligands help promote a biomimetic environment for photoencapsulated osteoblasts and, consequently, increase the production of an extracellular matrix in PEG hydrogels? The results presented herein specifically address these questions.

## 2. Experimental

### 2.1. Polymer synthesis and network formation

Poly(ethylene glycol)-diacrylate (PEGDA) was synthesized by dissolving PEG-4600 with triethylamine (1.1 M excess) in methylene chloride, adding acryloyl chloride (1.1 M excess) dropwise under nitrogen, and mixing for 24 h. The product was precipitated in diethyl ether, filtered, and dried in a dessicator. The product was redissolved in deionized water and dialyzed (Spectrum, 1000 MW cutoff) over several days with changes of deionized water to purify the product. Acryloyl-PEG-Arg-Gly-Asp (Acr-PEG-RGD) or Acryloyl PEG-Arg-Asp-Gly (Acr-PEG-RDG) was prepared as previously described [14]. Briefly, YRGDS or YRDGS (1 mg/ml, Bachem) was reacted with an equimolar amount of acryloyl-PEG-*N*-hydroxysuccinimide (3400 Da, Shearwater Polymers) in 50 mM sodium bicarbonate buffer (pH 8.2) for 2 h at room temperature. The macromer structures are shown in Fig. 1. All chemicals were obtained from Aldrich and used as received, unless noted otherwise.

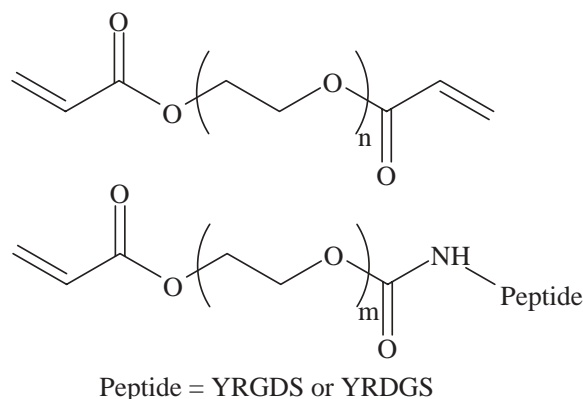


Fig. 1. Chemical structures of the multifunctional macromer PEGDA and monovinyl macromer acryloyl-PEG-Arg-Gly-Asp (Acr-PEG-RGD) used for hydrogel fabrication and osteoblast encapsulation.

## 2.2. Osteoblast harvest and culture

Osteoblasts were isolated from neonatal (<1-day-old) rat calvaria [16] to investigate both the attachment of osteoblasts on the surface of hydrogels and the function of encapsulated osteoblasts in hydrogel matrices. Briefly, the dissected calvaria was stripped of periosteum, minced with a scalpel, and incubated with Type I collagenase and trypsin for three consecutive 20 min digestions. The supernatant from the final digestion was filtered, and the cell pellet was suspended in Dulbecco's modified eagle medium (Gibco) supplemented with 10% FBS and 1% penicillin/streptomycin (Gibco). Osteoblasts after passage 3 were used in the current study.

## 2.3. RGD surface studies

Hydrogel disks (10 mm diameter and 1 mm thick before swelling) were fabricated with 10 wt% PEGDA in phosphate buffered saline (PBS) with the addition of no Acr-PEG-RGD, 0.5 mM Acr-PEG-RGD, 5.0 mM Acr-PEG-RGD, and 5.0 mM Acr-PEG-RDG. All hydrogels were fabricated by adding the PEGDA macromer and Acr-PEG-RGD to sterile PBS. An ultraviolet initiator, 2-hydroxy-1-[4-(hydroxyethoxy) phenyl]-2-methyl-1-propanone (D2959, Ciba Geigy) was added to this solution at a concentration of 0.05 wt% and polymerized in a sterile mold with  $\sim 4 \text{ mW/cm}^2$  ultraviolet light. These conditions were previously determined to be cytocompatible [17].

Osteoblasts were seeded onto sterile disks at a density of  $5 \times 10^4$  cells/cm<sup>2</sup>. After 2, 8, and 24 h, the disks were rinsed with PBS and phase contrast images (Nikon Eclipse TE300) were taken of the attached osteoblasts. Attached cells were counted on a minimum of three random fields (0.003 cm<sup>2</sup>) per disk ( $n = 3$  per composition). Cells were stained with hematoxylin to visualize the cell nucleus and aid in cell counting measurements. Cell spreading was quantified by measuring the area of the cells after 2 h of attachment. Using NIH Imaging software, the perimeter of the cell was outlined, and the area of cell attachment was quantified ( $\sim 2.1$  pixels/ $\mu\text{m}$ ).

After 12 h of culture on the hydrogel surfaces, osteoblasts were fixed in 4% formaldehyde in PBS for 10 min. The cells were permeabilized with 0.25% Triton X-100 in PBS for 10 min, and non-specific binding sites were blocked with 3% bovine serum albumin and 0.1% Tween-20 in PBS for 15 min at 37°C. The fixed cells were stained for actin with TRITC-conjugated phalloidin (1  $\mu\text{g/ml}$  in PBS) for 30 min at room temperature and rinsed with deionized water. Hydrogels were rinsed three times with PBS between each of the previous steps. Confocal microscopy (Zeiss Axioplan 2 Imaging System, LSM 5Pa) was used for imaging of actin filaments.

## 2.4. Viability of photoencapsulated osteoblasts

Osteoblasts were trypsinized from culture plates, counted, centrifuged, and suspended with the desired polymer solution at a concentration of  $50 \times 10^6$  cells/ml. Hydrogels synthesized from varying macromer compositions were analyzed and included: (1) 10 wt% PEGDA in PBS, (2) 20 wt% PEGDA in PBS, (3) 30 wt% PEGDA in PBS, (4) 10 wt% PEGDA in PBS with 0.5 mM Acr-PEG-RGD, and (5) 10 wt% PEGDA in PBS with 5.0 mM Acr-PEG-RGD. Forty microliters of the polymer-cell suspension was pipetted into a sterile cylindrical mold ( $\sim 5$  mm diameter, 2 mm thickness) and photopolymerized under ultraviolet light ( $\sim 4 \text{ mW/cm}^2$ ) for 5 min in a laminar flow hood. The cell/polymer construct was immediately removed from the mold and placed in media in a 24-well plate. The constructs were cultured on an orbital shaker (50 rpm) in an incubator (5% CO<sub>2</sub>, 37°C). After 1 day, the initial viability of encapsulated cells was determined using a LIVE/DEAD Viability/Cytotoxicity Kit (Molecular Probes, L-3224), which measures the membrane integrity of cells. Viable cells fluoresce green through the reaction of calcein AM with intracellular esterase, whereas non-viable cells fluoresce red due to the diffusion of ethidium homodimer across damaged cell membranes and binding with nucleic acids.

The long-term viability of photoencapsulated osteoblasts, as measured by mitochondrial activity, was analyzed with an MTT (3-[4,5-dimethylthiazol-2-yl]-2,5-diphenyltetrazolium bromide) assay (Sigma) after 1 day, 1 week, and 2 weeks of culture. A 1% MTT in serum-free media solution was added to each well containing the cell-hydrogel construct. Active mitochondria metabolize the tetrazolium salt to form an insoluble formazin dye. After 4 h of incubation, the constructs were placed in 1.5 ml polypropylene tubes, and 0.04 N HCl in spectrograde isopropanol was added. The constructs were broken apart using a tissue homogenizer and placed on an orbital shaker for 30 min for dissolution of the formazin. The absorbance was read with a spectrophotometer (Perkin Elmer Lambda 40) at 560 nm. All experiments were performed in triplicate.

## 2.5. *In vitro* analysis of mineralization

After 4 weeks of culture in media supplemented with 10 mM Na  $\beta$ -glycerol phosphate and 50  $\mu\text{g/ml}$  ascorbic acid on an orbital shaker (50 rpm), constructs (three per composition) were placed in a 10% formalin solution for 24 h, dehydrated, and paraffin embedded for histology using standard techniques. Histological sections were stained with a Von Kossa stain to visualize mineral deposits. Mineralized tissue formation was quantified using NIH Imaging software for a

minimum of five images from three samples for each composition.

## 2.6. Statistical analysis

Statistical analysis was performed using a Student's *t*-test with a minimum confidence level of 0.05 for statistical significance. All values are reported as the mean and standard deviation of the mean.

## 3. Results and discussion

In situ polymerized PEG-based hydrogels were investigated as matrices for the encapsulation of osteoblasts and the local delivery of cell–polymer constructs to bone defect sites. These gels were formed via a photoinitiated polymerization in the presence of a photoinitiator and an initiating light source. Potentially, a liquid macromer/cell suspension could be injected into the body through a needle and photopolymerized through the skin to provide a non-invasive technique to enhance bone regeneration. The transdermal polymerization of similar systems was previously investigated for injectable cartilage tissue engineering matrices [18] and for tissue adhesives [19]. The overall objective of this study was to investigate the influence of the hydrogel chemistry on the viability and activity of photoencapsulated osteoblasts and examine the potential of these cell–polymer constructs for the field of bone tissue engineering.

### 3.1. Osteoblast/hydrogel surface interactions

Due to low protein adsorption, PEG hydrogels do not facilitate the adhesion of cells, and thus, their applica-

tion to the field of tissue engineering has been limited. Here, the PEG hydrogels were modified homogeneously by copolymerizing a divinyl PEG (4600) macromer with a monovinyl PEG (3400) macromer modified with an adhesive peptide (i.e., RGD) to promote the attachment of rat calvarial osteoblasts. Hubbell and others [14] previously reported this chemistry and determined that a spacer was necessary between the acrylate group and peptide for cell recognition of the tethered peptide. Fig. 2 shows light micrographs of osteoblast attachment on hydrogel surfaces after 2 and 24 h. After 2 h, only rounded cells are seen on the unmodified gels, whereas, some cell spreading is seen on the 0.5 mM Acr-PEG-RGD and 5.0 mM Acr-PEG-RGD hydrogels. Cell spreading and density increased after 24 h on the modified hydrogels, yet the few cells observed on the unmodified hydrogels still maintain a rounded morphology. Osteoblasts attached to hydrogels modified with 5.0 mM-PEG-RGD (results not shown) had a similar morphology to the 10% PEGDA hydrogels, and thus, the enhanced attachment and spreading were attributed to the specificity of RGD in mediating cell adhesion.

The density of attached osteoblasts after 2, 8, and 24 h was quantified and is reported in Fig. 3. Only a small number of osteoblasts attached to the unmodified gels during this period, while the density of attached osteoblasts was much higher for the RGD-modified hydrogels. An increase in cell number was seen over this culture period for the modified hydrogels. Differences between the time points are attributed to both the attachment of additional cells from the initial cell suspension and some cell proliferation as the number of cells surpasses the initial seeding density for the 5.0 mM Acr-PEG-RGD. Additionally, a concentration dependence was noted, with the higher Acr-PEG-RGD

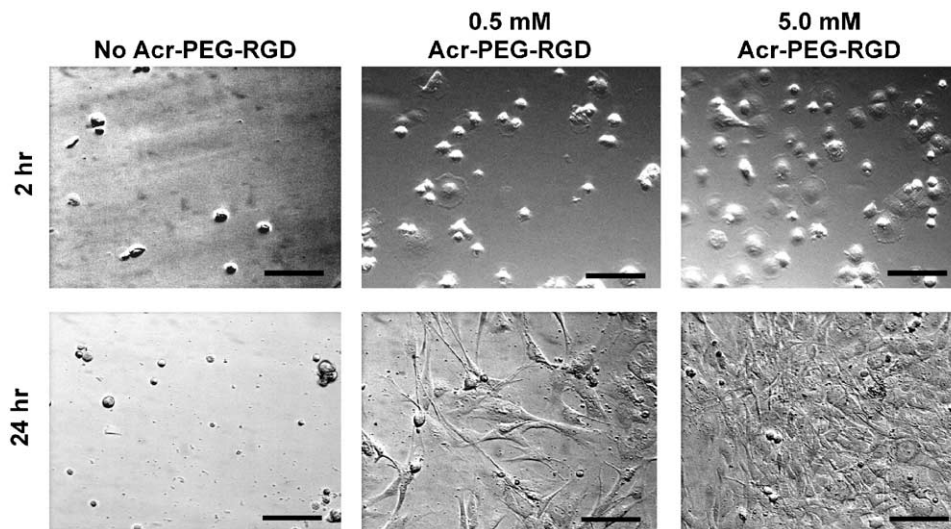


Fig. 2. Light micrographs of attached osteoblasts after 2 and 24 h for 10% PEGDA in PBS with no Acr-PEG-RGD, 0.5 mM Acr-PEG-RGD, and 5.0 mM Acr-PEG-RGD, bar = 50  $\mu$ m.

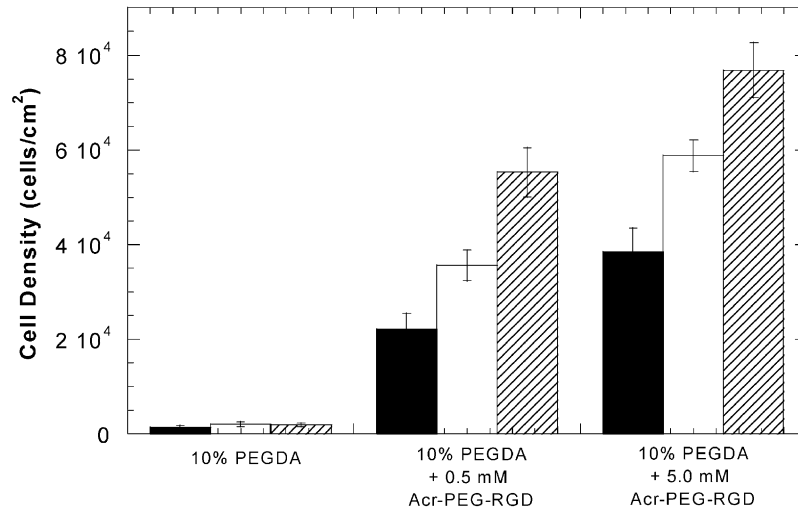


Fig. 3. Cell density of attached osteoblasts after 2 (black), 8 (white), and 24 (striped) h on 10% PEGDA in PBS with no Acr-PEG-RGD, 0.5 mM Acr-PEG-RGD, and 5.0 mM Acr-PEG-RGD. Values reported as the average of three random fields for a minimum of three hydrogels per composition (error bars designate standard deviation). Osteoblast densities are statistically significant ( $p < 0.001$ ) between the different compositions at each of the time points.

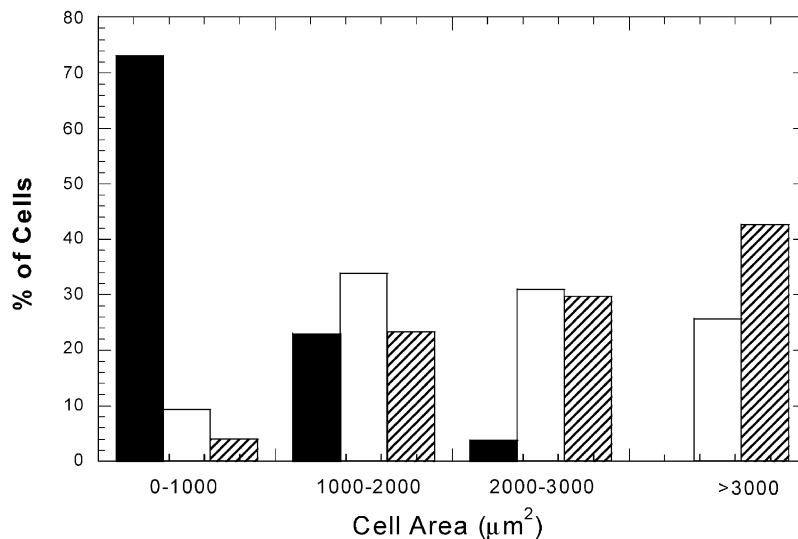


Fig. 4. Histogram of osteoblast spreading after 2 h of attachment on 10% PEGDA in PBS with no Acr-PEG-RGD (black), 0.5 mM Acr-PEG-RGD (white), and 5.0 mM Acr-PEG-RGD (striped). Values reported as the percentage of attached cells within a range of cell areas for three random fields on a minimum of three hydrogels per composition.

concentration facilitating a higher density of attached cells. For example, the cell density on the 5.0 mM Acr-PEG-RGD hydrogel was  $7.7 \pm 0.6 \times 10^4$  cells/cm<sup>2</sup> after 24 h of attachment, whereas the cell density was only  $5.5 \pm 0.5 \times 10^4$  cells/cm<sup>2</sup> for the 0.5 mM Acr-PEG-RGD-modified hydrogel. A statistical difference in cell number ( $p < 0.001$ ) was noted between the different Acr-PEG-RGD concentrations at each of the time points and between the different time points for the RGD-modified gels.

The spreading of attached osteoblasts was also dependent on the chemistry of the hydrogel surface. A histogram that reports the surface area of the attached

osteoblasts on the three hydrogel surfaces is shown in Fig. 4. The degree of cell spreading was classified by the surface area and placed in one of four categories: 0–1000 μm<sup>2</sup> (least spread), 1000–2000 μm<sup>2</sup>, 2000–3000 μm<sup>2</sup>, and > 3000 μm<sup>2</sup> (most spread). The histogram indicates that almost all of the attached cells on the unmodified hydrogel were rounded with very low cell spreading. As expected, the attached RGD ligand significantly influenced the attachment of cells, and specifically, the spreading of cells on hydrogel surfaces. Again, the concentration of RGD affected the spreading of cells with the highest density supporting the greatest degree of cell spreading, as measured by the cell surface

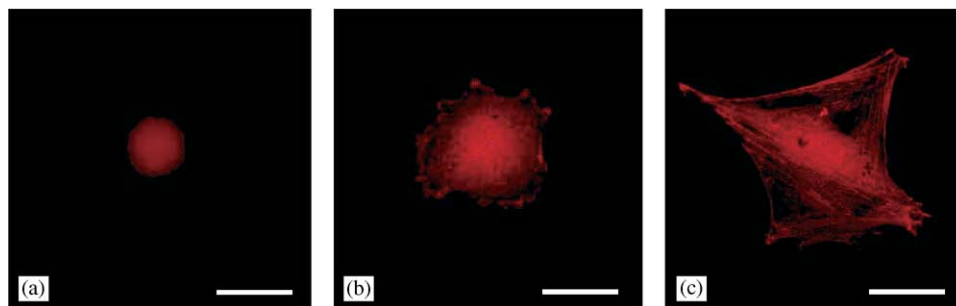


Fig. 5. Cytoskeleton organization observed with fluorescent confocal microscopy of actin-stained osteoblasts after 12 h on 10% PEGDA in PBS with no Acr-PEG-RGD (a), 0.5 mM Acr-PEG-RGD (b), and 5.0 mM Acr-PEG-RGD (c), bar = 20  $\mu\text{m}$ .

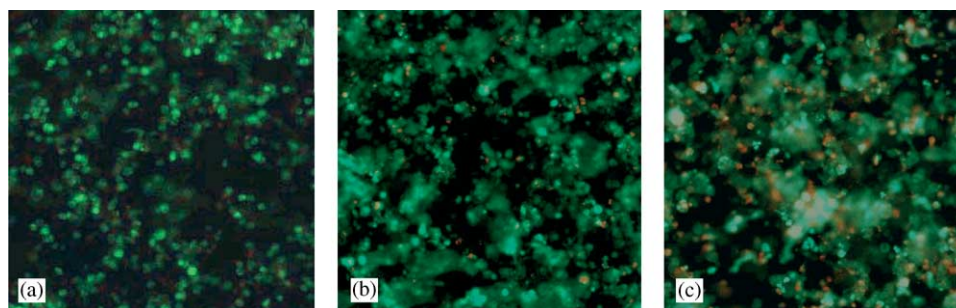


Fig. 6. Osteoblasts encapsulated in hydrogels formed from 10% PEGDA in PBS (a), 20% PEGDA in PBS (b), and 30% PEGDA in PBS (c) 24 h after encapsulation and stained with a LIVE/DEAD cell assay, where live cells fluoresce green and dead cells fluoresce red.

area. For example,  $\sim 42.7\%$  of the osteoblasts attached to hydrogels modified with 5.0 mM Acr-PEG-RGD spread to an effective area greater than  $3000 \mu\text{m}^2$ , but only  $\sim 25.7\%$  of cells on the 0.5 mM Acr-PEG-RGD hydrogel were within this range. The average cell area on these surfaces was  $780 \pm 440 \mu\text{m}^2$  for no Acr-PEG-RGD,  $2430 \pm 1260 \mu\text{m}^2$  for 0.5 mM Acr-PEG-RGD, and  $2920 \pm 1310 \mu\text{m}^2$  for 5.0 mM Acr-PEG-RGD.

As a final measure of the influence of adhesive peptide presence and concentration on osteoblast attachment and spreading on hydrogel surfaces, the cytoskeleton organization was examined after 12 h of attachment. Representative confocal images of actin staining of osteoblasts attached to the various surfaces are shown in Fig. 5. No organization of actin fibers was noted in the rounded osteoblasts on the unmodified surface or the low RGD density hydrogel, even though cell spreading is observed at this RGD concentration. Microfilament bundles were seen only in osteoblasts attached to the gel surface with the highest RGD concentration. This concentration dependence is similar to that reported by other investigators [20].

### 3.2. Photoencapsulation of osteoblasts in 3-dimensional hydrogel networks

Osteoblasts were mixed in liquid macromer/PBS solutions along with a cytocompatible photoinitiator and polymerized with low-intensity ultraviolet light.

Several hydrogel compositions were studied and included gels with the addition of adhesive peptides in various concentrations and gels synthesized from various initial macromer concentrations, which influences the overall crosslinking density of the network. Previous results [21] indicate that these networks reach complete conversion in  $< 5 \text{ min}$  and, thus, would polymerize on a clinically acceptable time scale. Fluorescent images of encapsulated osteoblasts 24 h after polymerization are shown in Fig. 6. Encapsulated osteoblasts were stained with a LIVE/DEAD assay, where live cells fluoresce green and dead cells fluoresce red. In the 10% PEGDA gel, the majority of osteoblasts are green, indicating cytocompatible initiation conditions. These results suggest that the photopolymerization environment is not detrimental to the initial viability of encapsulated osteoblasts. As the concentration of PEGDA increases, more red cells are seen, as well as an increase in cell aggregation. Furthermore, no macroscopic difference was seen in cell viability with the LIVE/DEAD assay between the unmodified- and RGD-modified 10% PEGDA hydrogels (results not shown). Bryant and Anseth [21] previously showed that the photoencapsulation of chondrocytes was possible for thick samples (up to 8 mm) without any loss of cell viability or significant light attenuation.

An MTT mitochondrial activity assay was used to determine the long-term viability of osteoblasts

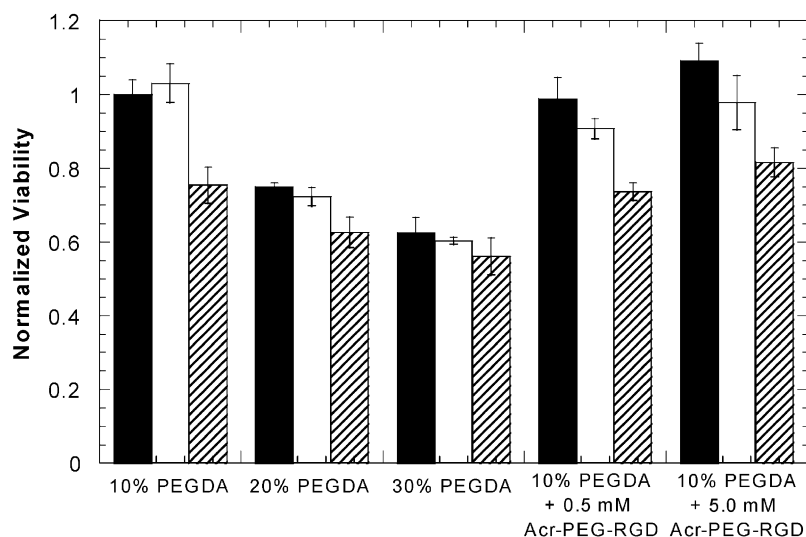


Fig. 7. Viability of osteoblasts encapsulated in hydrogels synthesized from 10% PEGDA in PBS (a), 20% PEGDA in PBS (b), 30% PEGDA in PBS (c), 10% PEGDA in PBS with 0.5 mM Acr-PEG-RGD (d), and 10% PEGDA in PBS with 5.0 mM Acr-PEG-RGD after 1 day (black), 1 week (white), and 2 weeks (striped) determined with an MTT viability assay. Values reported as the average of three constructs per composition (error bars designate standard deviation). There is a statistical difference ( $p < 0.05$ ) in osteoblast viability between the different macromer concentrations.

encapsulated in PEG hydrogels. The results, shown in Fig. 7, were normalized to the viability of osteoblasts encapsulated in a 10% PEGDA hydrogel 24 h after encapsulation. This system had the highest initial cell viability with the LIVE/DEAD assay. In general, the higher macromer concentrations had a lower initial viability when compared to the 10% PEGDA hydrogels, whereas the RGD-modified gels produced similar results. The normalized viability was  $1.03 \pm 0.05$  for the 10% PEGDA gel after 1 week of culture, but only  $0.72 \pm 0.02$  and  $0.60 \pm 0.01$  for the 20% PEGDA and 30% PEGDA hydrogels, respectively. These values are statistically different ( $p < 0.05$ ) at all three time points (1 day, 1 week, and 2 weeks). An increase in macromer concentration leads to an increase in radical concentration during polymerization and a more highly cross-linked network, which could lead to transport limitations for nutrients to the encapsulated cells. Both of these factors could lead to a decrease in cell viability. There was no statistical difference ( $p > 0.05$ ) between the unmodified and modified 10 wt% hydrogels, indicating that the incorporated RGD has no detrimental affect on the viability of encapsulated osteoblasts. A trend of decreasing viability is noted for all hydrogel compositions after 1 and 2 weeks of in vitro culture. This decrease may be attributed in part, to limited diffusion in these gels, especially as extracellular matrix components are being produced by encapsulated osteoblasts. This limited diffusion could also limit the diffusion of the MTT tetrazolium salt to the encapsulated cells and result in a reported viability lower than the actual viability.

### 3.3. Mineralization by photoencapsulated osteoblasts

Von Kossa-stained histological sections of photoencapsulated osteoblasts in PEG hydrogels after 4 weeks of in vitro culture are shown in Fig. 8. This staining procedure stains mineral deposits brown to black. As expected, mineral deposits are localized in the area immediately adjacent to the encapsulated cells. In these non-degradable networks, diffusion of collagen and subsequent mineralization are limited and, thus, tissue formation is limited. A hydrogel that degrades in a manner that matches extracellular matrix production may be optimal for these applications. These gels are easily modified with degradable linkages [22] of lactic acid and caprolactone for tailored degradation rates.

Enhanced mineralization was present in the hydrogels with tethered adhesive peptides, with the highest mineralization in the gels with the highest RGD concentration. Mineralization was quantified as  $14.5 \pm 3.8\%$  of the image for no Acr-PEG-RGD,  $24.8 \pm 3.7\%$  for 0.5 mM Acr-PEG-RGD, and  $38.5 \pm 4.5\%$  for 5.0 mM Acr-PEG-RGD. These values are all statistically different ( $p < 0.001$ ). Reznia and Healy [23] reported a similar dependence of mineralization by osteoblasts to surfaces on peptide density. Potentially, the presence of adhesive peptides allows for a more natural environment for the anchorage-dependent osteoblasts, and thus, mineral deposition by the osteoblasts is increased. The production of a mineralized matrix by these suspended osteoblasts is a significant result and indicates that these networks may find applications for bone regeneration.

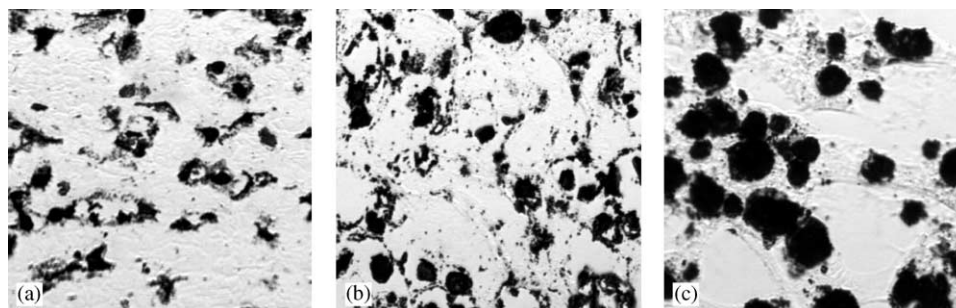


Fig. 8. Von Kossa-stained histological sections (5  $\mu$ m) after 4 weeks in vitro culture of osteoblasts encapsulated in hydrogels formed from 10% PEGDA in PBS with no Acr-PEG-RGD (a), 0.5 mM Acr-PEG-RGD (b), and 5.0 mM Acr-PEG-RGD (c). Mineralization was quantified and values were statistically different ( $p < 0.001$ ) for the different Acr-PEG-RGD concentrations.

In a recent review of injectable biodegradable materials for orthopedic tissue engineering, Temenoff and Mikos [24] outlined several requirements for these materials. Specifically, the authors stated that injectable materials must be biocompatible and have non-toxic degradation products, have sufficient mechanical properties for the intended application, promote tissue formation, be sterilizable to prevent infection, polymerize on a clinically acceptable time scale with a minimal temperature change, and promote ease of handling by a surgeon. This study has shown that the encapsulation of osteoblasts in a hydrogel using multifunctional macromers and a photoinitiated polymerization has potential to fulfill these requirements for certain orthopedic applications. While the mechanics of these hydrogel networks may not be sufficient for large defects in a load-bearing bone, these materials and techniques may be appropriate for craniofacial bone defects. Additionally, these hydrogels may be desirable for composite implants, where the hydrogel is used to fill the pores in a load-bearing scaffold with better mechanical properties.

#### 4. Conclusions

Hydrogels were modified with RGD adhesive peptides that enhanced the attachment, spreading, and cytoskeletal organization of rat calvarial osteoblasts on polymer surfaces that are otherwise non-adhesive. Osteoblasts were successfully photoencapsulated in PEG hydrogels and remained viable depending on the initial macromer concentration. As a final investigation of this procedure for bone tissue engineering, encapsulated osteoblasts formed a mineralized matrix, which was enhanced in gels containing the adhesive peptides. These systems have potential as an injectable in situ forming material that could be reacted via a transdermal photopolymerization.

#### Acknowledgements

The authors gratefully acknowledge funding from the National Institute of Health (AR44375-02), the Dreyfus

Foundation, and the US Department of Education's Graduate Assistantships in Areas of National Need program for a fellowship for J.A.B. Additionally, the authors would like to acknowledge the laboratory assistance of Ryan Bender.

#### References

- [1] Bauer TW, Muschler GF. Bone graft materials—an overview of the basic science. *Clin Orthop* 2000;371:10–27.
- [2] Lane JM, Tomin E, Bostrom MP. Biosynthetic bone grafting. *Clin Orthop* 1999;367S:S107–17.
- [3] Dee KC, Bizios R. Mini-review: proactive biomaterials and bone tissue engineering. *Biotech Bioeng* 1996;50:438–42.
- [4] Jefferis CD, Lee AJC, Ling RSM. Thermal aspects of self-curing poly(methyl methacrylate). *J Bone Jt Surg* 1975;57B:511–8.
- [5] Peter SJ, Nolley JA, Widmer MS, Merwin JE, Yaszemski MJ, Yasko AW, Engel PS, Mikos AG. In vitro degradation of a poly(propylene fumarate)/beta-tricalcium phosphate composite orthopaedic scaffold. *Tissue Eng* 1995;1:41–52.
- [6] Peter SJ, Kim P, Yasko AW, Yaszemski MJ, Mikos AG. Crosslinking characteristics of an injectable poly(propylene fumarate)/beta-tricalcium phosphate paste and mechanical properties of the crosslinked composite for use as a biodegradable bone cement. *J Biomed Mater Res* 1999;44:314–21.
- [7] Svaldi-Muggli D, Burkoth AK, Anseth KS. Crosslinked polyanhydrides for use in orthopaedic applications: degradation behavior and mechanics. *J Biomed Mater Res* 1998;46:271–8.
- [8] Burkoth AK, Burdick J, Anseth KS. Surface and bulk modifications to photocrosslinked polyanhydrides to control degradation behavior. *J Biomed Mater Res* 2000;51:352–9.
- [9] Burdick JA, Peterson AJ, Anseth KS. Conversion and temperature profiles during the photoinitiated polymerization of thick orthopaedic biomaterials. *Biomaterials* 2001;22:1779–86.
- [10] Dee KC, Andersen TT, Bizios R. Osteoblast migration characteristics on substrates modified with immobilized adhesive peptides. *Biomaterials* 1999;20:221–7.
- [11] Reznia A, Healy KE. Biomimetic peptide surfaces that regulate adhesion, spreading, cytoskeletal organization, and mineralization of the matrix deposited by osteoblast-like cells. *Biotechnol Prog* 1999;15:19–32.
- [12] Rowley JA, Madlambayan G, Mooney DJ. Alginate hydrogels as synthetic extracellular matrix materials. *Biomaterials* 1999;20:45–53.
- [13] Stile RA, Healy KE. Thermo-responsive peptide-modified hydrogels for tissue regeneration. *Biomacromolecules* 2001;2:185–94.

- [14] Hern DL, Hubbell JA. Incorporation of adhesion peptides into nonadhesive hydrogels useful for tissue resurfacing. *J Biomed Mater Res* 1998;39:266–76.
- [15] Mann BK, Gobin AS, Tsai AT, Schmedlen RH, West JL. Smooth muscle cell growth in photopolymerized hydrogels with cell adhesive and proteolytically degradable domains: synthetic ECM analogs for tissue engineering. *Biomaterials* 2001;22:3045–51.
- [16] Ishaug SL, Yaszemski MJ, Bizios R, Mikos AG. Osteoblast function on synthetic biodegradable polymers. *J Biomed Mater Res* 1994;28:1445–53.
- [17] Bryant SJ, Nuttelman CR, Anseth KS. Cytocompatibility of UV and visible light photoinitiating systems on cultured NIH/3T3 fibroblasts in vitro. *J Biomater Sci Polym E* 2000;11:439–57.
- [18] Elisseeff J, Anseth K, Sims D, McIntosh W, Randolph M, Langer R. Transdermal photopolymerization for minimally invasive implantation. *Proc Natl Acad Sci* 1999;96:3104–7.
- [19] Bryant S, Martens P, Elisseeff J, Randolph M, Langer R, Anseth KS. Trans-tissue photopolymerization of poly(vinyl alcohol) hydrogels. In: Stokke BT, Elgsaeter, editors. *Chemical and physical network formation and control of properties*, West Sussex, UK: Wiley, 1999. p. 396–403.
- [20] Massia SP, Hubbell JA. Covalent surface immobilization of Arg-Gly-Asp and Tyr-Ile-Gly-Ser-Arg containing peptides to obtain well-defined cell-adhesive substrates. *Anal Biochem* 1990;187:292–301.
- [21] Bryant SJ, Anseth KS. The effects of scaffold thickness on tissue engineered cartilage in photocrosslinked poly(ethylene oxide) hydrogels. *Biomaterials* 2001;22:619–26.
- [22] Sawhney AS, Pathak CP, Hubbell JA. Bioerodible hydrogels based on photopolymerized poly(ethylene glycol)-co-poly( $\alpha$ -hydroxy acid) diacrylate macromers. *Macromolecules* 1993;26:581–7.
- [23] Reznia A, Healy KE. The effect of peptide surface density on mineralization of a matrix deposited by osteogenic cells. *J Biomed Mater Res* 2000;52:595–600.
- [24] Temenoff JS, Mikos AG. Injectable biodegradable materials for orthopedic tissue engineering. *Biomaterials* 2000;21:2405–12.